Distributed Joint Observation and Transmission Planning Method for Multiple Agile Satellites in Mega Constellation Networks

Ningxuan Guo, Yuqi Wang, Yufei Li, Liang Liu, Yupeng Gong, Ningyuan Wang, Anshou Li, Dan Liu, and Xiaoqing Zhong

***Abstract*—With the improvement of satellites' maneuverability, agile earth observation satellites (AEOSs) can pitch and roll themselves to observe targets with longer visible time window (VTW), which enables more targets to be observed while bringing greater uncertainties of mission planning and more conflicts of resources. Meanwhile, mega constellation networks (MCNs) provide powerful tools to transmit massive observation data. In MCNs, AEOSs can observe targets agilely and access communication satellites (CSs) by inter-satellite links (ISLs) to offload data. Based on this architecture, we propose a Distributed Joint Observation and Transmission Planning method for Multiple AEOSs (MA-DJOTP). This method uses a targets allocation strategy, a CS allocation model, and a targets reallocation strategy to transform the multi-AEOS problem into several single-AEOS subproblems. The Single-AEOS Joint Observation and Transmission Planning (SA-JOTP) model is formulated as a Mixed Integer Quadratic Constraint Programming (MIQCP) problem based on a mission-based time slot division method, which can help simplify the observation time determination and ISL handover modeling. The SA-JOTP model can realize both the benefit maximization and the transmission delay minimization based on practical constraints of mission transition time, laser ISLs' characteristics, and limited onboard resources. We verify the effectiveness of the proposed MA-DJOTP algorithm in MCNs with 720 CSs and 3, 16, 36, 360 AEOSs. The results show that the proposed algorithm can obtain a solution very close to the global optimum of the centralized method and is applicable in MCNs with hundreds of satellites.**

***Index Terms*—Agile earth observation satellites, observation and transmission mission planning, mega constellation networks, inter-satellite links, distributed algorithm.**

I. Introduction

Earth observation satellites (EOSs) can observe targets and transmit their data back to earth, which are vital in disaster emergency rescue, environmental monitoring, and meteorology [1]. The observation and transmission mission planning of EOSs has a great impact on the effectiveness of space observation systems.

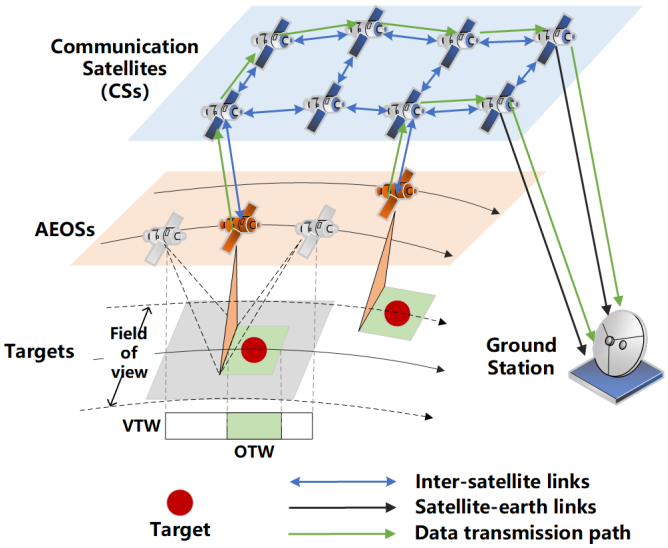

Fig. 1. Architecture of AEOSs' observation and data transmission in constellation networks.

As the improvement of EOSs' maneuverability, agile earth observation satellites (AEOSs) are produced. Traditional non-agile EOSs can only observe targets when flying over them, while AEOSs can pitch and roll themselves to observe before or after flying over targets so that more missions can be executed [2]. When an AEOS can observe a target, the AEOS is in the visible time window (VTW) of the target. The exact imaging time is considered as the observation time window (OTW), as shown in Fig. 1. For non-agile EOSs, the OTW is the same as the VTW. While for AEOSs, the exact OTW needs to be determined in the VTW, which leads to greater uncertainties. Besides, the long VTWs of AEOSs result in more data to offload, more complexity of mission transition, and more conflicts of resources.

Meanwhile, many AEOSs can generate a large amount of data, which will put higher demands on data transmission. Communication satellites (CSs) can form a network (eg. Starlink [3], OneWeb [4]) to provide powerful tools to transmit massive observation data. In this paper, we consider a mega constellation network (MCN) shown in Fig. 1. CSs can help transmit data back to Earth through inter-satellite

This work was supported in part by the 173 Plan Domain Foundation under Grant 2023-JCJQ-JJ-0491. *(Corresponding author: Xiaoqing Zhong.)*

Ningxuan Guo, Yupeng Gong, and Anshou Li are with the Department of Strategic and Advanced Interdisciplinary Research, Peng Cheng Laboratory, Shenzhen, Guangdong 518055, China (e-mail: gnx@zju.edu.cn; gyphit@163.com; liash@pcl.ac.cn).

Yuqi Wang, Liang Liu, Ningyuan Wang, Dan Liu, and Xiaoqing Zhong are with the Institute of Telecommunication and Navigation Satellites, China Academy of Space Technology, Beijing 100094, China (e-mail: wangyuqi_its@163.com; liuliang1945@buaa.edu.cn; ningyuan.wang@foxmail.com; hellodanielle@163.com; hitzxq@126.com).

Yufei Li is with the Advanced Research Institute of Multidisciplinary Sciences, Beijing Institute of Technology, Beijing 100081, China (e-mail: liyufeibit@163.com).

links (ISLs) and satellite-earth links. AEOSs only need to observe targets agilely and access CSs concurrently to offload data. Consequently, timely transmission of massive data can be achieved.

Due to the rapid development of MCN and satellite platforms, it becomes more challenging for mission planning of AEOSs. On this issue, research efforts can be classified into three aspects.

The first aspect focuses on **the observation planning of AEOSs, while not considering the offload of the image data**. Many research [2], [5], [6] made efforts on the "time-dependent transition time", which results from the fact that each pair of consecutive missions requires a transition time to maneuver the look angle of the AEOS from the previous target to the next target. Besides, Han et al. [7] studied the cloud coverage uncertainty in the multi-AEOS scheduling problem. He et al. [8] solved the AEOS scheduling problem by a genetic Markov decision process and the reinforcement learning method. Du et al. [9] proposed a task assignment strategy based on a probability prediction model to divide the multi-AEOS problem into several single-AEOS subproblems.

The second aspect focuses on **the data transmission in MCN based on the time-varying topology**. In this aspect, the snapshot graph is widely applied to divide the time domain evenly into several time slots and consider the network topology to be static during a time slot. Zhou et al. [10] proposed a benefits maximization method in terms of sum weighted transmitted data volume. Yan et al. [11], [12] optimized the ISLs' topology to achieve the maximum throughput and the minimization of transmission delay. Guo et al. [13] proposed a distributed task-aware topology optimization method in a double-layered MCN to realize the maximization of data transmission benefits.

However, the above two aspects only studied one of the observation or transmission missions. The separation scheduling results in the low efficiency of AEOS' mission performance. In practice, observation and transmission missions have strong coupling features since they share the same time domain and are both related to the onboard storage and energy resources. But few works studied **the joint observation and transmission scheduling of AEOSs**, which is the focus of this paper belonging to the third aspect.

In the third aspect, Zhang et al. [14] proposed a mixed integer programming model to formulate the imaging and data downloading scheduling problem. However, this paper only considered the data transmission to ground stations and did not include ISL in MCNs. To the best of the authors' knowledge, He et al. [15] first studied the joint observation and transmission scheduling algorithm for AEOSs (i.e. JOTSAS) in satellite networks. The JOTSAS aims to realize more imaging data to be collected and offloaded. However, it is a centralized method that is hard to solve in MCNs with hundreds of satellites. Besides, JOTSAS has some problems such as the complex transition time modeling, the lack of connection between data transmission and ISLs, the lack of optimization in transmission delay, and the lack of consideration for limited onboard resources.

Motivated by [15] and the development of ISL in MCNs, we propose a Distributed Joint Observation and Transmission Planning method for Multi-AEOSs (MA-DJOTP) in MCNs. In this paper, we consider the ISLs as laser links and consider the same AEOS AS-01 as in [2], [5], [6], whose look angles are fixed during an observation mission. Comparison of JOTSAS in [15] and the proposed MA-DJOTP is listed in TABLE I. We propose a mission-based time slot division method to simplify the modeling of the complex transition time constraint. To make the algorithm applicable in MCNs, we also propose targets and CSs allocation strategies to transform the multi-AEOSs scheduling problem into single-AEOS subproblems and solve them in parallel.

TABLE I
COMPARISON OF JOTSAS IN [15] AND THE PROPOSED MA-DJOTP

	JOTSAS [15]	MA-DJOTP (proposed)
Architecture	Centralized	Distributed
Time slot division	Same for observation and transmission	Different for observation and transmission (mission-based)
Transmission mission transition	Transitions are required between the transmission of any different target data	Transitions are required between any different ISL linking objects
Modeling of transition time constraint	Complex	Simplified based on the mission-based time slot division method
Objective	Benefit maximization	Benefit maximization and transmission delay minimization
Limited energy and storage resources	Not considered	Considered
MCNs	Not applicable	Applicable

Compared to the state of the art, the main contributions of this paper can be summarized as follows:

- A mission-based time slot division method that has different time slot durations for observation and transmission mission planning. This method can help simplify the OTW determination and the ISLs' transition time modeling.
- A Single-AEOS Joint Observation and Transmission Planning (SA-JOTP) model, which is formulated as a Mixed Integer Quadratic Constraint Programming (MIQCP) problem. This model gives practical constraints considering the mission transition time, laser ISLs' characteristics, and limited onboard resources. It realizes both the benefits maximization and the transmission delay minimization.
- A distributed algorithm (i.e. MA-DJOTP) for multiple AEOSs based on a targets allocation strategy with the ranking of AEOSs, a CS allocation model, a targets reallocation strategy, and the parallel solving of the SA-JOTP problems of each AEOS. This algorithm can obtain a solution very close to the global optimum of the centralized method and is applicable in MCNs with hundreds of satellites.

The rest of this paper is organized as follows. Section II presents the system model with the assumptions, some symbol definitions, and the mission-based time slot division method.

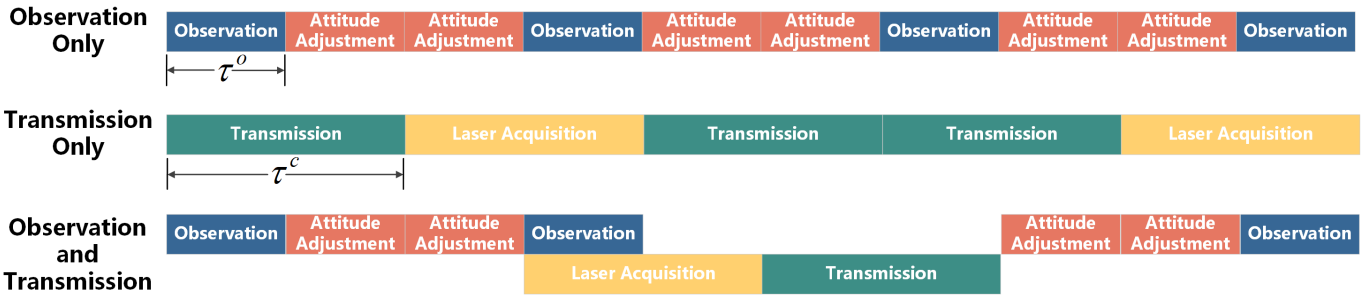

Fig. 2. Planning observation and transmission for an AEOS in the time domain with the mission-based time slot division method.

Section III formulates the SA-JOTP model as an MIQCP problem with constraints and the multi-objective function. In Section IV, we propose an observation targets allocation method, a CS allocation method, and a targets reallocation method to form the distributed algorithm MA-DJOTP with the proposed SA-JOTP. Then, we verify the effectiveness of the proposed methods in MCNs with 720 CSs and 3, 16, 36, 360 AEOSs in Section V. At last, Section VI concludes this paper and discusses future work.

II. System Model

In this section, we give the system model assumptions, symbol definitions, and the mission-based time slot division method in turn.

A. Assumptions

This study mainly focuses on the observation and transmission joint planning method for AEOSs. Therefore, some assumptions are made to simplify the problem:

1) This study only considers spot targets with one-pass observation. The observation duration for each target is considered a constant value.
2) The attitude transition time between observing different targets is considered a constant value.
3) The studied AEOS AS-01 does not adjust attitude during an observation mission.
4) This study considers the data transmission through ISLs from AEOSs to CSs. We will decide on the optimal ISLs for AEOs to optimize the transmission. The routing among CSs and from CSs to ground stations is not considered.
5) The laser acquisition time between connecting to different CSs by ISLs is considered a constant value.
6) The energy and storage resource management is taken into account.

B. Definitions

In this multi-layer system with multiple targets, multiple AEOSs, and multiple CSs, we define some indices and sets to distinguish different nodes.

1) Index:

- i: index of AEOSs. The number of AEOS is N^a.
- k: index of targets. The number of targets is N^o.
- j: index of CSs. The number of CSs is N^c.
- t: index of time slots.

2) Sets:

- $\mathcal{V}^o_{i,K}$: The set of all visible targets of AEOS i during the planning horizon, where the number of elements is $|\mathcal{V}^o_{i,K}| = N^o_i$, satisfying $\sum_{i=1}^{N^a} N^o_i = N^o$.
- $\mathcal{V}^a_{I,k}$: The set of all AEOSs that can observe target k within the planning horizon, where the number of elements is $|\mathcal{V}^a_{I,k}| = N^a_k$, satisfying $\sum_{k=1}^{N^o} N^a_k = N^a$.
- $\mathcal{V}^c_{i,J}$: The set of all CSs that can connect to AEOS i by ISLs during the planning horizon, where the number of elements is $|\mathcal{V}^c_{i,J}| = N^c_i$, satisfying $\sum_{i=1}^{N^a} N^c_i = N^c$.
- $\mathcal{V}^a_{I,j}$: The set of all AEOSs that can connect to CS j by ISLs during the planning horizon, where the number of elements is $|\mathcal{V}^a_{I,j}| = N^a_j$, satisfying $\sum_{j=1}^{N^c} N^a_j = N^a$.
- $\mathcal{T}^o$: The set of observation time slots, where the number of elements is $|\mathcal{T}^o| = T^o$, each time slot duration is τ^o.
- $\mathcal{T}^c$: The set of transmission time slots, where the number of elements is $|\mathcal{T}^c| = T^c$, each time slot duration is τ^c.

C. Mission-based Time Slot Division Method

In the snapshot graph, the network topology is considered unchanged during a time slot. Since we need to make the optimal decision with the unit of time slot, the duration of a time slot determines the number of variables and the optimization complexity. A long time slot can reduce complexity but may lose some optimality of the solution. While a too short time slot may result in a too huge problem to be solved.

To reduce the solving complexity while ensuring the solution performance, we propose a mission-based time slot division method, which is shown in Fig. 2. The main ideas are as follows:

1) The time slot duration for observation and transmission are different.
2) The observation time slot duration τ^o is equal to the time needed for observing one target.
3) The transmission time slot duration τ^c is equal to the time needed for laser acquisition when executing ISL handover.
4) The time slot duration τ^o and τ^c have an integer multiple relationship, so they can be unified with multiple or division operations.

For **observation** missions, the observation duration is generally shorter than the needed attitude transition duration [2], [7], so making τ^o be equal to the observation duration is

practical. The advantage of diving time domain with τ^o is: for each mission, once an observation time slot is determined, the specific observing start and end time is determined. Thus, the observation-related decision variables can be defined as discrete integer variables in time domain. This will greatly reduce the difficulty of problem modeling and solving.

For **transmission** missions, dividing time domain with τ^c can reduce the nonlinear coupling relationship of time domain. Since only one time slot is needed when performing ISL handover, so when determining the link state of a certain time slot, only the link state of its previous time slot need to be considered. Thus, the ISL handover constraint can be modeled by the state difference between adjacent time slots. This will greatly simplify the modeling of the ISL handover constraint and reduce the solving complexity.

For **joint observation and transmission**, there are some interacting constraints between these two missions. As shown in the third case of Fig. 2, the AEOS can not execute ISL handover and data transmission when adjusting attitude due to the stable requirements of the satellite for laser acquisition and ISL maintenance. Therefore, for modeling the interacting constraints, the time slots τ^o and τ^c should be able to convert to each other. The mapping between the time slots is as follows:

$$\gamma = \frac{\tau^c}{\tau^o} \tag{1}$$

$$t \in \mathcal{T}^o \rightarrow \left\lceil \frac{t}{\gamma} \right\rceil \in \mathcal{T}^c \tag{2}$$

$$t \in \mathcal{T}^c \rightarrow [(t-1)\gamma + 1, t \cdot \gamma] \in \mathcal{T}^o \tag{3}$$

III. Problem Formulation of a single AEOS

In this section, we will propose the SA-JOTP model for a single AEOS i. The considered targets are in set $\mathcal{V}^o_{i,K}$, and CSs are in set $\mathcal{V}^c_{i,J}$. We will formulate the constraints of observation, transmission, the relation between observation and transmission, satellite transition state, energy, and storage in turn. At last, a linear weighted multi-objective optimization problem will be formulated for the single AEOS.

A. Observation Mission Constraints

1) Related Decision Variables:

- $\boldsymbol{\psi}_i = \{\boldsymbol{\psi}_i(k,t) | k \in \mathcal{V}^o_{i,K}, t \in \mathcal{T}^o\} \in \mathbb{R}^{N^o_i \times T^o}$: a 0-1 observation decision matrix, where its element $\boldsymbol{\psi}_i(k,t)$ is '1' when the AEOS i decides to observe target k at time slot t, and '0' the opposite.
- $x_{i,k}$: a 0-1 scalar variable to represent whether target k is scheduled to be observed by AEOS i.
- $p_{k,k'}$: a 0-1 scalar variable whose value is '1' when target k' is observed after k, and '0' the opposite, where $k \neq k'$.

Constraints on the value range of decision variables are:

$$\boldsymbol{\psi}_i(k,t),\ x_{i,k},\ p_{k,k'} \in \{0,1\} \quad \forall k \neq k' \in \mathcal{V}^o_{i,K}, \forall t \in \mathcal{T}^o \tag{4}$$

2) Target Visibility: Define $\boldsymbol{O}_i \in \mathbb{R}^{N^o_i \times T^o}$ be the visible matrix of AEOS i, where its element $\boldsymbol{O}_i(k,t)$ is '1' when k is in the visible range of i at time slot t, and '0' the opposite. We can calculate this parameter matrix $\boldsymbol{O}_i$ according to the pitch and roll ability of AEOS. The matrix $\boldsymbol{O}_i$ is an integer expression of the VTW. Assume $[a_{i,k}, e_{i,k}]$ is the VTW between AEOS i and target k, then for $\forall t \in [a_{i,k}, e_{i,k}]$, $\boldsymbol{O}_i(k,t) = 1$.

To guarantee AEOS i can only observe targets when they are visible, the visibility constraint can be described as:

$$\boldsymbol{\psi}_i \leq \boldsymbol{O}_i \tag{5}$$

3) Number of Observed Targets: We assume each AEOS has one camera, so it can only observe one target at a time slot:

$$\sum_{k \in \mathcal{V}^o_{i,K}} \boldsymbol{\psi}_i(k,t) \leq 1 \quad \forall t \in \mathcal{T}^o \tag{6}$$

4) Observation Duration: Since the time slot duration τ^o is equal to the observation mission duration, we only need to arrange a time slot for each target observation. It means the observation duration $l^o = 1$. That is, when k is scheduled to be observed, $x_{i,k}$ and the observation duration both equal to 1, which can be expressed as:

$$\sum_{t \in \mathcal{T}^o} \boldsymbol{\psi}_i(k,t) = x_{i,k} \quad \forall k \in \mathcal{V}^o_{i,K} \tag{7}$$

5) Observation Transition: Since an AEOS needs to adjust its attitude to point at a target, two targets can not be observed continuously. Let Δ^o be the necessary attitude transition duration between adjacent observation missions, then Δ^o/τ^o is the needed number of time slots. We use the Big-M model [16] with associated constant M to formulate the observation transition constraint as follows:

$$\sum_{t \in \mathcal{T}^o} [\boldsymbol{\psi}_i(k,t) \cdot t] - \sum_{t \in \mathcal{T}^o} \left[\boldsymbol{\psi}_i(k',t) \cdot \left(t + l^o + \frac{\Delta^o}{\tau^o} \right) \right] \geq -M \cdot p_{k,k'} \quad \forall k, k' \in \mathcal{V}^o_{i,K}, k \neq k' \tag{8}$$

$$p_{k,k'} + p_{k',k} = 1 \tag{9}$$

The above formulas realize the logical relation as:

$$\text{if} \sum_{t \in \mathcal{T}^o} [\boldsymbol{\psi}_i(k,t) \cdot t] - \sum_{t \in \mathcal{T}^o} \left[\boldsymbol{\psi}_i(k',t) \cdot \left(t + l^o + \frac{\Delta^o}{\tau^o} \right) \right] \leq 0,$$
$$\text{then} \quad p_{k,k'} = 1,\ p_{k',k} = 0$$

where $\sum_{t \in \mathcal{T}^o} [\boldsymbol{\psi}_i(k,t) \cdot t]$ obtains the observation time of k, and $\sum_{t \in \mathcal{T}^o} \left[\boldsymbol{\psi}_i(k',t) \cdot \left(t + l^o + \frac{\Delta^o}{\tau^o} \right) \right]$ obtains the earliest observation time after observing k'. If k does not satisfy the condition of observing after k', then k should be observed before k' with $p_{k,k'} = 1$. Note that if k is not observed, then $p_{k,k'} \equiv 1$ if k' is observed.

B. Transmission Mission Constraints

1) Related Decision Variables:

- $\boldsymbol{\delta}_i = \{\boldsymbol{\delta}_i(j,t) | j \in \mathcal{V}^c_{i,J}, t \in \mathcal{T}^c\} \in \mathbb{R}^{N^c_i \times T^c}$: a 0-1 linking decision matrix, where its element $\boldsymbol{\delta}_i(j,t)$ is '1' when the AEOS i connects to CS j by an ISL at time slot t, and '0' the opposite.
- $\boldsymbol{\beta}_i = \{\boldsymbol{\beta}_i(k,t) | k \in \mathcal{V}^o_{i,K}, t \in \mathcal{T}^c\} \in \mathbb{R}^{N^o_i \times T^c}$: a 0-1 transmission decision matrix, where its element $\boldsymbol{\beta}_i(k,t)$ is '1' when the AEOS i **starts** to transmit observation data of target k at time slot t, and '0' the opposite.

- $st_{i,k} \in \mathcal{T}^o$: an integer variable to represent target k's data transmission start time expressed in $\mathcal{T}^o$.

Constraints on the value range of decision variables are:

$$\boldsymbol{\delta}_i(j,t), \boldsymbol{\beta}_i(k,t) \in \{0,1\} \quad \forall j \in \mathcal{V}_{i,J}^c, k \in \mathcal{V}_{i,K}^o, t \in \mathcal{T}^c \quad (10)$$

2) ISL Connectivity: Define $\boldsymbol{S}_i \in \mathbb{R}^{N_i^c \times T^c}$ be the connectable matrix between AEOS i and all CSs at all time slots, where its element $\boldsymbol{S}_i(j,t)$ is '1' when CS j is connectable to AEOS i at time slot t, and '0' the opposite. This parameter matrix $\boldsymbol{S}_i$ can be calculated according to antenna angle and relative velocity of satellites [13]. AEOS i can only establish ISLs with connectable CSs, which can be described as:

$$\boldsymbol{\delta}_i \leq \boldsymbol{S}_i \quad (11)$$

3) Number of ISLs: We assume each AEOS has one inter-satellite communication antenna, so it can only connect to one CS at a time slot:

$$\sum_{j \in \mathcal{V}_{i,J}^c} \boldsymbol{\delta}_i(j,t) \leq 1 \quad \forall t \in \mathcal{T}^c \quad (12)$$

4) Transmission Time: As $\boldsymbol{\beta}_i(k,t)$ represents the transmission start time slot, then for each observed target k, we need to select one time slot for this target data to start transmitting. This constraint can be expressed as:

$$\sum_{t \in \mathcal{T}^c} \boldsymbol{\beta}_i(k,t) = x_{i,k} \quad \forall k \in \mathcal{V}_{i,K}^o \quad (13)$$

Meanwhile, the selected transmission start time should not be too late so that all data of the observed target can be transmitted. Assume the data amount generated by observing each target is q^o, the data transmission rate of ISL is v^c, then the needed number of time slot for transmitting each target data is $l^c = \lceil q^o/(v^c \cdot \tau^c) \rceil$. Therefore, data transmission should not start at the last $l^c - 1$ time slot:

$$\sum_{k \in \mathcal{V}_{i,K}^o} \boldsymbol{\beta}_i(k,t) = 0 \quad \forall t \in [T^c - l^c + 2, T^c] \quad (14)$$

With constraints (13) and (14), we make sure that once a target is observed, all of its data should be offloaded within the planning horizon.

5) Relation of ISLs and Data Transmission: Observation data can be transmitted only when an ISL is available. If we decide to start transmitting data at $t - l^c + 1$, then the l^c time slots in $[t - l^c + 1, t]$ should have available ISLs. That is:

$$\text{if} \sum_{k \in \mathcal{V}_{i,K}^o} \boldsymbol{\beta}_i(k, t - l^c + 1) = 1,$$
$$\text{then} \sum_{j \in \mathcal{V}_{i,J}^c} \boldsymbol{\delta}_i(j, t - l^c + 1) = 1, \cdots, \sum_{j \in \mathcal{V}_{i,J}^c} \boldsymbol{\delta}_i(j,t) = 1.$$

In other words:

$$\text{if} \sum_{t - l^c + 1}^{t} \sum_{k \in \mathcal{V}_{i,K}^o} \boldsymbol{\beta}_i(k,t) = 1, \text{ then } \sum_{j \in \mathcal{V}_{i,J}^c} \boldsymbol{\delta}_i(j,t) = 1.$$

This constraint can be formulated as:

$$\sum_{j \in \mathcal{V}_{i,J}^c} \boldsymbol{\delta}_i(j,t) \geq \begin{cases} \sum_{t'=1}^{t} \sum_{k \in \mathcal{V}_{i,K}^o} \boldsymbol{\beta}_i(k,t'), & \forall t \in [1, l^c - 1] \\ \sum_{t'=t-l^c+1}^{t} \sum_{k \in \mathcal{V}_{i,K}^o} \boldsymbol{\beta}_i(k,t'), & \forall t \in [l^c, T^c] \end{cases} \quad (15)$$

Note that this constraint is based on the assumption that at most one target data can be transmitted by an ISL at a time slot, and the data transmission for a target is continuous.

6) ISL Handover: Since an AEOS needs to adjust the antenna to point at a CS for laser acquisition, a necessary duration for ISL handover is necessary. As introduced in Section II-C, the handover duration Δ^c is equal to the time slot duration τ^c. So we need to guarantee that there is at least one time slot between linking with different CSs.

Define $\boldsymbol{d\delta}_i(j,t) = \boldsymbol{\delta}_i(j,t) - \boldsymbol{\delta}_i(j,t-1)$ be the link state difference between adjacent time slots t and $t-1$, where $\boldsymbol{\delta}_i(j,0)$ represents the initial link state between i and j. Let $\boldsymbol{d\delta}_i(t) = [\boldsymbol{d\delta}_i(1,t), \cdots, \boldsymbol{d\delta}_i(j,t), \cdots]^\mathsf{T} \in \mathbb{R}^{N_i^c}$ be the link state difference vector with N_i^c CSs. Different cases of the link state difference are listed in TABLE II.

TABLE II
DIFFERENT CASES OF THE LINK STATE DIFFERENCE

Cases (for a certain $t \in \mathcal{T}^c$)	Value of $\boldsymbol{d\delta}_i(j,t)$	Norm of $\boldsymbol{d\delta}_i(t)$
Continuously Link	$\{0\}$	0
Disconnect Link	$\{-1, 0\}$	1
Establish Link	$\{1, 0\}$	1
Handover with no interval	$\{1, -1, 0\}$	$\sqrt{2}$

According to TABLE II, to avoid link handover with no interval (i.e. $\boldsymbol{\delta}_i(j, t-1) = \boldsymbol{\delta}_i(j', t) = 1$ with $j \neq j'$), the norm of the link difference vector $\boldsymbol{d\delta}_i(t)$ should be less than or equal to 1, which can be expressed as:

$$|\boldsymbol{d\delta_i}(t)| \leq 1 \quad \forall t \in \mathcal{T}^c \quad (16)$$

C. Relation Constraints of Observation and Transmission

For each target k, data transmission should not be earlier than observation, which can be formulated as:

$$st_{i,k} - \sum_{t \in \mathcal{T}^o} [\boldsymbol{\psi}_i(k,t) \cdot t] \geq 0 \quad \forall k \in \mathcal{V}_{i,K}^o \quad (17)$$

where the data transmission start time slot $st_{i,k} \in \mathcal{T}^o$ can be calculated by $\boldsymbol{\beta}_i(k,t)$ as follows:

$$st_{i,k} = \left[\left(\sum_{t \in \mathcal{T}^c} [\boldsymbol{\beta}_i(k,t) \cdot t] - 1 \right) \gamma + 1 \right] \cdot x_{i,k} \quad \forall k \in \mathcal{V}_{i,K}^o \quad (18)$$

where $\sum_{t \in \mathcal{T}^c} [\boldsymbol{\beta}_i(k,t) \cdot t]$ can obtain the transmission start time slot expressed in $\mathcal{T}^c$, and γ is used to transform the time slot into $\mathcal{T}^o$. Here, $x_{i,k}$ is multiplied to guarantee the value of $st_{i,k}$ be 0 when the target k is not observed or transmitted.

D. Satellite Transition State Constraints

1) Related Decision Variables:

- $\xi_{i,t}$: A 0-1 scalar variable to represent whether AEOS i is adjusting attitude at time slot t, where $t \in \mathcal{T}^o$.
- $\lambda_{i,t}$: A 0-1 scalar variable to represent whether AEOS i is performing laser acquisition (ISL handover) at time slot t, where $t \in \mathcal{T}^c$.

Constraints on the value range of decision variables are:

$$\xi_{i,t} \in \{0,1\},\ \forall t \in \mathcal{T}^o \quad \lambda_{i,t} \in \{0,1\},\ \forall t \in \mathcal{T}^c \tag{19}$$

2) Attitude Adjustment State: Before each observation, Δ^o/τ^o time slots are required for attitude adjustment. That is, for a certain time slot $t \in \mathcal{T}^o$:

$$\text{if} \sum_{k \in \mathcal{V}^o_{i,K}} \boldsymbol{\psi}_i(k,t) = 1,$$
$$\text{then } \xi_{i,t-\Delta^o/\tau^o} = 1, \xi_{i,t-\Delta^o/\tau^o+1} = 1, \cdots, \xi_{i,t-1} = 1.$$

In other words:

if one of the elements in set

$$\left\{ \sum_{k \in \mathcal{V}^o_{i,K}} \boldsymbol{\psi}_i(k,t+1), \cdots, \sum_{k \in \mathcal{V}^o_{i,K}} \boldsymbol{\psi}_i(k,t+\frac{\Delta^o}{\tau^o}) \right\} \text{ is 1,}$$

then $\xi_{i,t} = 1$.

This constraint can be formulated as:

$$\xi_{i,t} = \begin{cases} \sum\limits_{t'=t+1}^{t+\frac{\Delta^o}{\tau^o}} \sum\limits_{k \in \mathcal{V}^o_{i,K}} \boldsymbol{\psi}_i(k,t'), & \forall t \in \left[1, T^o - \frac{\Delta^o}{\tau^o}\right] \\ 0, & \text{otherwise.} \end{cases} \tag{20}$$

3) Laser Acquisition State: For each AEOS, Before establishing an ISL with a CS, $\Delta^c/\tau^c = 1$ time slot is required for laser acquisition. That is:

$$\text{if} \sum_{j \in \mathcal{V}^c_{i,J}} \boldsymbol{d\delta}_i(j,t) = 1,\ \text{then } \lambda_{i,t-1} = 1,\ \text{else } \lambda_{i,t-1} = 0$$

Recall that $\boldsymbol{d\delta}_i(j,t)$ represents the link state difference between adjacent time slots $t-1$ and t, so $\boldsymbol{d\delta}_i(j,t) = 1$ indicates that an ISL is established with j at time slot t. The constraint for the laser acquisition state $\lambda_{i,t}$ is formulated as:

$$\lambda_{i,t} = \begin{cases} \frac{1}{2} \sum\limits_{j \in \mathcal{V}^c_{i,J}} \boldsymbol{d\delta}_i(j,t+1) \left(\sum\limits_{j \in \mathcal{V}^c_{i,J}} \boldsymbol{d\delta}_i(j,t+1) + 1 \right), \\ \qquad\qquad \forall t \in [1, T^c - 1] \\ 0, \qquad\qquad \text{otherwise.} \end{cases} \tag{21}$$

According to TABLE II, the value of $\sum_{j \in \mathcal{V}^c_{i,J}} \boldsymbol{d\delta}_i(j,t+1)$ can be -1 or 1, so we multiply the item $\sum_{j \in \mathcal{V}^c_{i,J}} \boldsymbol{d\delta}_i(j,t+1) + 1$ to guarantee that $\lambda_{i,t}$ can only be 0 or 1.

4) State Exclusivity: Laser acquisition and ISL maintenance have certain requirements for the stability of the satellite platform. Therefore, when the satellite is adjusting attitude, laser acquisition and data transmission of ISL can not be performed. It means that the attitude adjustment state and the laser acquisition state or ISL connecting state are exclusive. These constraints can be formulated as:

$$1 - \lambda_{i,\lceil t/\gamma \rceil} \geq \xi_{i,t} \quad \forall t \in \mathcal{T}^o \tag{22}$$

$$1 - \sum_{j \in \mathcal{V}^c_{i,J}} \boldsymbol{\delta}_i(j, \lceil t/\gamma \rceil) \geq \xi_{i,t} \quad \forall t \in \mathcal{T}^o \tag{23}$$

where $\lceil t/\gamma \rceil$ is the round up of t/γ, which is performed to transform the time slot from $\mathcal{T}^c$ to $\mathcal{T}^o$.

5) ISL Continuity: To avoid unnecessary ISL handover, we hope the ISLs are as continuous as possible. That is, if the current time slot has established an ISL, then the next time slot should keep this ISL if the linking CS is still connectable and the AEOS does not adjust attitude. This constraint can be expressed as:

$$\boldsymbol{\delta}_i(j,t+1) \geq \boldsymbol{\delta}_i(j,t) \boldsymbol{S}_i(j,t+1) \left(1 - \sum_{t \cdot \gamma + 1}^{(t+1)\gamma} \xi_{i,t} \right) \ \forall t \leq T^c - 1 \tag{24}$$

where γ is multiplied when sum $\xi_{i,t}$ to transform the time slot from $\mathcal{T}^o$ to $\mathcal{T}^c$.

E. Energy Constraints

1) Related Decision Variables:

- $E^C_{i,t}$: a scalar variable to represent the consumed energy amount of AEOS i during time slot t, where $t \in \mathcal{T}^c$.
- $E^H_{i,t}$: a scalar variable to represent the harvested energy amount by solar panels of AEOS i during time slot t, where $t \in \mathcal{T}^c$.
- $E_{i,t}$: a scalar variable to represent the remaining onboard energy of AEOS i at the end of time slot t, where $t \in \mathcal{T}^c$.

2) Energy Consumption: The energy is consumed by five parts: observation with constant power P^o, attitude adjustment with power P^a, laser acquisition with power P^l, data transmission with power P^t, and some other conventional operations with power P^r. Therefore, the energy consumption during each time slot $t \in \mathcal{T}^c$ is:

$$E^C_{i,t} = \tau^o \cdot \sum_{t'=(t-1)\gamma+1}^{t \cdot \gamma} \left[P^o \sum_{k \in \mathcal{V}^o_{i,K}} \boldsymbol{\psi}_i(k,t') + P^a \cdot \xi_{i,t'} \right] + \tau^c \cdot \left[P^l \cdot \lambda_{i,t} + P^t \sum_{j \in \mathcal{V}^c_{i,J}} \boldsymbol{\delta}_i(j,t) + P^r \right] \ \forall t \in \mathcal{T}^c \tag{25}$$

where γ is used for transforming the time slot expressed in $\mathcal{T}^o$ into $\mathcal{T}^c$.

3) Energy Harvesting: For each AEOS, the harvested energy during each time slot should not exceed the maximum amount harvested during the sunlight duration. Let P^H be the output power of solar panels, and $l^s_{i,t} \in [0, \tau^c]$ be the sunlight duration within time slot t. Then, this constraint can be formulated as:

$$0 \leq E^H_{i,t} \leq P^H \cdot l^s_{i,t} \quad \forall t \in \mathcal{T}^c \tag{26}$$

4) Energy Equilibrium and Capacity: The amount of energy variation per time slot is equal to the amount of harvested energy minus the consumed energy during this time slot:

$$E_{i,t} - E_{i,t-1} = E_{i,t}^{H} - E_{i,t}^{C} \quad \forall t \in \mathcal{T}^c \tag{27}$$

where $E_{i,0}$ is the initial onboard energy.

At each time slot, the onboard energy should not exceed the maximum battery capacity $E_i^{\max}$ and the maximum discharge depth θ, which can be expressed as:

$$E_i^{\max}(1-\theta) \le E_{i,t} \le E_i^{\max} \quad \forall t \in \mathcal{T}^c \tag{28}$$

F. Storage Constraints

1) Related Decision Variables:

- $b_{i,t}$: a scalar variable to represent the data amount stored on AEOS i at the end of time slot t, where $t \in \mathcal{T}^c$.

2) Flow Equilibrium: The amount of data storage variation per time slot is equal to the amount of generated observation data minus the transmitted data during this time slot. Recall that the data amount of observing each target is q^o, and with the observing duration $l^o = 1$, the generated data amount during a time slot in $\mathcal{T}^o$ is also q^o. The average transmitted data amount during a time slot in $\mathcal{T}^c$ is $q^c = q^o/l^c$. Let $b_{i,0}$ be the initial data amount stored onboard. The flow equilibrium constraint is formulated as (29), which is at the bottom of this page.

In both cases of this formula, the first term calculates the generated data amount during one time slot in $\mathcal{T}^c$, so the generated data during $[(t-1)\gamma+1, t\cdot\gamma]$ is summed for $\boldsymbol{\psi}_i(k,t)$ to transform the time slot set. The second item calculates the transmitted data amount during a time slot in $\mathcal{T}^c$. Since $\boldsymbol{\beta}_i(k,t)$ is the start transmission time, so any target data transmission starts from $[t-l^c+1, t]$ (or $[1,t]$ in the second case) will result in data outflow at this time slot t.

3) Storage Capacity: At each time slot, the stored data amount should not exceed the maximum memory capacity $B_i^{\max}$. The onboard storage amount constraint can be expressed as:

$$0 \le b_{i,t} \le B_i^{\max} \quad \forall t \in \mathcal{T}^c \tag{30}$$

G. Optimization Problem Formulation

For each AEOS i, the objective of the observation and transmission planning problem is to jointly maximize the benefits while minimizing the transmission delay. Let ω_k be the benefit of observing and transmitting data of target k. We use the linear weighting method [17] to formulate the multi-objective optimization problem SA-JOTP as follows:

$$\max \ \alpha_1 \frac{\sum\limits_{k\in\mathcal{V}_{i,K}^o} \omega_k \cdot x_{i,k}}{\sum\limits_{k\in\mathcal{V}_{i,K}^o} \omega_k} - \alpha_2 \frac{\sum\limits_{k\in\mathcal{V}_{i,K}^o} \omega_k \cdot st_{i,k}}{T^o \cdot N_i^o} \quad \forall i \in [1, N^a] \tag{31}$$

subject to:

$$(1), (4) \sim (30)$$

where α_1 and α_2 are the weights of the two objectives.

In (31), the first item realizes the maximization of benefits, where the numerator calculates the total benefits obtained by observing target k and transmitting its data, and the denominator is the maximum benefits value used for normalization. The second item realizes the minimization of transmission delay, where the numerator calculates the sum of the weighted transmission start time, and the denominator is also used for normalization.

This problem has integer decision variables $\boldsymbol{\psi}_i$, $x_{i,k}$, $p_{k,k'}$, $\boldsymbol{\delta}_i$, $\boldsymbol{\beta}_i$, $st_{i,k}$, $\xi_{i,t}$, $\lambda_{i,t}$ and continuous variables $E_{i,t}^C$, $E_{i,t}^H$, $E_{i,t}$, $b_{i,t}$. Constraints (18), (21), and (24) have multiplication operations between variables, so they are quadratic constraints. Other constraints are all linear. Therefore, (31) is an MIQCP problem.

Theorem 1. *In problem (31), the value of α_1 and α_2 should meet $\alpha_1/\alpha_2 \ge \overline{\omega}_k$, where $\overline{\omega}_k$ is the average benefit of targets.*

Proof. To achieve the objectives of (31), we need to guarantee that the objective function value of $x_{i,k} = 1$ is always greater than that of $x_{i,k} = 0$. That is:

$$\alpha_1 \frac{\omega_k}{\sum_{k\in\mathcal{V}_{i,K}^o} \omega_k} - \alpha_2 \frac{\omega_k \cdot st_{i,k}}{T^o \cdot N_i^o} > 0 \quad \forall k \in \mathcal{V}_{i,K}^o \tag{32}$$

By derivation, we have:

$$\frac{\alpha_1}{\alpha_2} > \frac{st_{i,k} \cdot \sum_{k\in\mathcal{V}_{i,K}^o} \omega_k}{T^o \cdot N_i^o} = \frac{st_{i,k} \cdot \overline{\omega}_k}{T^o} \quad \forall k \in \mathcal{V}_{i,K}^o \tag{33}$$

Since the maximum value of $st_{i,k}$ can be approximated as T^o, we can obtain:

$$\frac{\alpha_1}{\alpha_2} > \max\left\{ \frac{st_{i,k}\cdot\overline{\omega}_k}{T^o} \middle| k \in \mathcal{V}_{i,K}^o \right\} \approx \overline{\omega}_k \tag{34}$$

□

IV. Distributed Solution Algorithm

In this Section, we propose an observation targets allocation method, a CS allocation strategy, and a targets reallocation method in turn. Then, we form the proposed methods and

$$b_{i,t} - b_{i,t-1} = \begin{cases} \sum\limits_{t'=(t-1)\gamma+1}^{t\cdot\gamma} \sum\limits_{k\in\mathcal{V}_{i,K}^o} \boldsymbol{\psi}_i(k,t') \cdot q^o - \sum\limits_{t'=t-l^c+1}^{t} \sum\limits_{k\in\mathcal{V}_{i,K}^o} \boldsymbol{\beta}_i(k,t') \cdot q^c, & \forall t \in [l^c, T^c] \\ \sum\limits_{t'=(t-1)\gamma+1}^{t\cdot\gamma} \sum\limits_{k\in\mathcal{V}_{i,K}^o} \boldsymbol{\psi}_i(k,t') \cdot q^o - \sum\limits_{t'=1}^{t} \sum\limits_{k\in\mathcal{V}_{i,K}^o} \boldsymbol{\beta}_i(k,t') \cdot q^c, & \forall t \in [1, l^c - 1] \end{cases} \tag{29}$$

the SA-JOTP model into a distributed algorithm for multiple AEOSs, named MA-DJOTP.

A. Observation Targets Allocation

1) Allocation Process: If each AEOS is completely autonomous in observing targets without interacting, then some targets might be observed many times and some targets may not be observed. Therefore, for mission planning of single AEOS, we firstly need to allocate all observation targets to their appropriate AEOSs. The allocation process aims to make each target have great possibility to be observed and allocate all targets as evenly as possible.

Define $\boldsymbol{A} = \{\boldsymbol{A}(k,i)|\forall k, \forall i\} \in \mathbb{R}^{N^o \times N^a}$ be a 0-1 matrix to represent the target allocation result, where its element $\boldsymbol{A}(k,i) = 1$ when target k is allocated to i. Let $\boldsymbol{L} = \{\boldsymbol{L}(k)|\forall k\} \in \mathbb{R}^{N^o}$ be the 0-1 vector to label whether each target has been allocated.

The allocation process is expressed in pseudo-code as a function $\boldsymbol{A} = Tar\_allocation()$ in Algorithm 1. The three crucial steps of the allocation process can be summarized as:

Step 1. First allocation: for each target k, if it is visible to only one AEOS during the planning horizon (i.e. $|\mathcal{V}^a_{I,k}| = 1$), allocate k to this AEOS and label k as allocated with $\boldsymbol{L}(k) = 1$. Meanwhile, if a target is not visible to any AEOSs, we also let $\boldsymbol{L}(k) = 1$ to avoid repeated visits to this target in the program.

Step 2. Second allocation: for each AEOS i, if the number of visible targets is below average (i.e. $|\mathcal{V}^o_{i,K}| \leq \frac{N^o}{N^a}$), then all visible targets are allocated to this AEOS. This step is to ensure the uniformity of allocation.

Step 3. Formal allocation: for each target k that has not yet been allocated, rank all AEOSs that can observe k and allocate k to the top-ranked AEOS.

Algorithm 1: Allocate all observation targets to respective AEOSs: function $\boldsymbol{A} = Tar\_allocation()$.

Input: Paramters of all targets and all AEOSs.
Output: The target allocation results.

```
Initialize A ← 0^{N^o × N^a}, L ← 0^{N^o × 1}
for k = 1 : N^o do                          // First allocation
    if |V^a_{I,k}| = 1 then
        A(k, V^a_{I,k}) ← 1;   // allocate k to V^a_{I,k}
        L(k) ← 1;              // label k as allocated
    else
        if |V^a_{I,k}| = 0 then L(k) ← 1 ;
    end
end
for i = 1 : N^a do                          // Second allocation
    if (1 ≤ |V^o_{i,K}| ≤ N^o/N^a) and (L(V^o_{i,K}) = 0) then
        A(V^o_{i,K}, i) ← 1;   // allocate V^o_{i,K} to i
        L(V^o_{i,K}) ← 1;
    end
end
for k = 1 : N^o do                          // Formal allocation
    if L(k) = 0 then
        R_k ← Rank(A, V^a_{I,k});          // rank AEOSs
        A(k, R_k(1)) ← 1;// allocate k to the
         top-ranked AEOS
    end
end
return A
```

2) Rank of AEOSs: In the target allocation process, the rank of AEOSs plays a vital role, as introduced in step 18 in Algorithm 1. For each target k, all AEOSs that can observe k should be ranked. We propose a rank mechanism with four items. Each item has a rank value of 0∼1, so the maximum total rank value is 4. The top-ranked AEOS has the smallest rank value.

Define $\boldsymbol{R}_k = \{\boldsymbol{R}_k(i)|\forall i \in \mathcal{V}^a_{I,k}\} \in \mathbb{R}^{N^a_k}$ be the rank value vector of all AEOSs that can observe target k, where $\boldsymbol{R}_k(i)$ is the rank value of AEOS i. The four rank items $\boldsymbol{R}^1_k(i)$, $\boldsymbol{R}^2_k(i)$, $\boldsymbol{R}^3_k(i)$, $\boldsymbol{R}^4_k(i)$ for $\forall i \in \mathcal{V}^a_{I,k}$ are described as follows.

VTW: the earlier observation, the better ranking. For some emergency missions, we hope the targets can be observed as early as possible, so we prefer to allocate targets to those AEOSs that can observe them earlier. Recall that $a_{i,k}$ is the start time of VTW between AEOS i and target k. The rank value of this item can be calculated by:

$$\boldsymbol{R}^1_k(i) = \frac{a_{i,k}}{\sum_{i \in \mathcal{V}^a_{I,k}} a_{i,k}} \tag{35}$$

where the denominator is used to scale the rank value to 0∼1 and make $\sum_{i \in \mathcal{V}^a_{I,k}} \boldsymbol{R}^1_k(i) = 1$.

Note that if $a_{i,k} > T^o - \frac{\Delta^c + l^c \cdot \tau^c}{\tau^o} + 1$ for a certain AEOS, which means the observation and transmission can not be finished in the planning horizon, then a big rank value M will be given to i to avoid allocating k to this AEOS.

Observation distance: the closer the distance, the better the ranking. Let $d_{i,k}$ be the closest distance between AEOS i and target k in the VTW. Generally, a smaller value of $d_{i,k}$ means the target k is closer to the ground tracks of AEOS i so that a better image quality can be obtained. The rank value of this item can be calculated by:

$$\boldsymbol{R}^2_k(i) = \frac{d_{i,k}}{\sum_{i \in \mathcal{V}^a_{I,k}} d_{i,k}} \tag{36}$$

Number of allocated targets: the fewer targets that have been allocated to this AEOS, the better ranking. We hope each AEOS to be allocated a similar number of targets so that more targets can be observed. This rank value can be calculated by:

$$\boldsymbol{R}^3_k(i) = \frac{\sum_{k \in \mathcal{V}^o_{i,K}} \boldsymbol{A}(k,i)}{\sum_{i \in \mathcal{V}^a_{I,k}} \sum_{k \in \mathcal{V}^o_{i,K}} \boldsymbol{A}(k,i)} \tag{37}$$

Note that in step 18 of Algorithm 1, the rank function is called in the for-loop with the input variable $\boldsymbol{A}$, so the allocation result of the subsequent targets is constantly adjusted according to the previous allocation result.

Conflict degree to allocated targets: the fewer conflicting VTWs of allocated targets, the better ranking. For each target k' allocated to AEOS i (i.e. $\boldsymbol{A}(k',i) = 1$), if the VTW of k is overlapped with that of k', then the VTW of k and k'

are considered conflicting. Recall that $[a_{i,k}, e_{i,k}]$ is the VTW between AEOS i and target k, then the VTW of k and k' are overlapped when $a_{i,k'} \leq a_{i,k} \leq e_{i,k'}$ or $a_{i,k'} \leq e_{i,k} \leq e_{i,k'}$. Let $N_{i,k}^{con}$ be the number of conflicting VTWs between k and all targets k' that have been allocated to AEOS i. A smaller value of $N_{i,k}^{con}$ means this target k is more likely to be observed if allocated to AEOS i. The rank value can be calculated by:

$$\boldsymbol{R}_k^4(i) = \frac{N_{i,k}^{con}}{\sum_{i \in \mathcal{V}_{I,k}^a} N_{i,k}^{con}} \tag{38}$$

The rank function $\boldsymbol{R}_k = Rank(\boldsymbol{A}, \mathcal{V}_{I,k}^a)$ is described in Algorithm 2.

B. Communication Satellites Allocation

In MCNs, there are hundreds of CSs. It is difficult for each AEOS to choose an appropriate one among all CSs while planning observation missions. Therefore, to reduce the complexity of single-AEOS mission planning while avoiding the link conflict among AEOSs, we need to allocate appropriate CSs to AEOSs for data transmission during the planning horizon.

We propose a CS allocation method based on an Integer Linear Programming (ILP) model, which aims to achieve full link coverage of each AEOS during the planning horizon with a minimum number of CSs. This method is applicable in MCNs with an adequate number of CSs.

Define $\boldsymbol{C} = \{\boldsymbol{C}(j,i) | \forall j, \forall i\} \in \mathbb{R}^{N^c \times N^a}$ be a 0-1 decision matrix to represent the CS allocation result, where its element $\boldsymbol{C}(j,i) = 1$ when CS j is allocated to AEOS i. The ILP problem is named as function $\boldsymbol{C} = Com\_allocation()$ and is formulated as:

$$\min \sum_{i=1}^{N^a} \sum_{j=1}^{N^c} \boldsymbol{C}(j,i) \tag{39}$$

subject to:

$$\sum_{j=1}^{N^c} [\boldsymbol{C}(j,i) \cdot \boldsymbol{S}_i(j,t)] \geq 1 \quad \forall t \in \mathcal{T}^c, \ \forall i \in [1, N^a] \tag{40}$$

$$\sum_{i=1}^{N^a} \boldsymbol{C}(j,i) \leq 1 \quad \forall j \in [1, N^c] \tag{41}$$

$$\boldsymbol{C}(j,i) \in \{0,1\} \quad \forall j \in [1, N^c], \ \forall i \in [1, N^a] \tag{42}$$

where the objective function (39) is to minimize the total number of allocated CSs; inequality (40) guarantees that each AEOS i has connectable CSs at each time slot t; inequality (41) ensures that each CS is only allocated to one AEOS; (42) indicates the decision variables are binary.

C. Reallocation of Unscheduled Observation Targets

After the mission planning of each AEOS by solving the SA-JOTP problem, some allocated targets may not be scheduled to be observed (i.e. $\boldsymbol{A}(k,i) = 1$, but $x_{i,k} = 0$). Therefore, we propose a reallocation method to enable more targets to be observed.

Define $\boldsymbol{A}' = \{\boldsymbol{A}'(k,i) | \forall k, \forall i\} \in \mathbb{R}^{N^o \times N^a}$ be a 0-1 matrix to represent the target reallocation result. Let set $\mathcal{U}$ to mark the AEOSs that have changed the target allocation result.

Algorithm 2: Rank of all AEOSs that can observe target k: function $\boldsymbol{R}_k = Rank(\boldsymbol{A}, \mathcal{V}_{I,k}^a)$.

Input: The current target allocation result $\boldsymbol{A}$; the parameters of AEOSs in set $\mathcal{V}_{I,k}^a$
Output: The rank values $\boldsymbol{R}_k$ of AEOSs in set $\mathcal{V}_{I,k}^a$

for $\forall i \in \mathcal{V}_{I,k}^a$ **do** // Calculate $N_{i,k}^{con}$
  $N_{i,k}^{con} \leftarrow 0$;
  for $k' \in \{k' | \boldsymbol{A}(k',i) = 1\}$ **do**
    if $(a_{i,k'} \leq a_{i,k} \leq e_{i,k'})$ *or* $(a_{i,k'} \leq e_{i,k} \leq e_{i,k'})$ **then** $N_{i,k}^{con} = N_{i,k}^{con} + 1$;
  end
end
for $\forall i \in \mathcal{V}_{I,k}^a$ **do** // Calculate $\boldsymbol{R}_k(i)$
  if $a_{i,k} > T^o - \frac{\Delta^c + l^c \cdot \tau^c}{\tau^o} + 1$ **then**
    $\boldsymbol{R}_k(i) \leftarrow M$;
  else
    $\boldsymbol{R}_k^1(i) \leftarrow \frac{a_{i,k}}{\sum_{i \in \mathcal{V}_{I,k}^a} a_{i,k}}$; $\boldsymbol{R}_k^2(i) \leftarrow \frac{d_{i,k}}{\sum_{i \in \mathcal{V}_{I,k}^a} d_{i,k}}$;
    $\boldsymbol{R}_k^3(i) \leftarrow 0$; $\boldsymbol{R}_k^4(i) \leftarrow 0$;
    if $\sum_{i \in \mathcal{V}_{I,k}^a} \sum_{k \in \mathcal{V}_{i,K}^o} \boldsymbol{A}(k,i) \neq 0$ **then**
      $\boldsymbol{R}_k^3(i) \leftarrow \frac{\sum_{k \in \mathcal{V}_{i,K}^o} \boldsymbol{A}(k,i)}{\sum_{i \in \mathcal{V}_{I,k}^a} \sum_{k \in \mathcal{V}_{i,K}^o} \boldsymbol{A}(k,i)}$;
    if $\sum_{i \in \mathcal{V}_{I,k}^a} N_{i,k}^{con} \neq 0$ **then**
      $\boldsymbol{R}_k^4(i) \leftarrow \frac{N_{i,k}^{con}}{\sum_{i \in \mathcal{V}_{I,k}^a} N_{i,k}^{con}}$;
    $\boldsymbol{R}_k(i) \leftarrow \boldsymbol{R}_k^1(i) + \boldsymbol{R}_k^2(i) + \boldsymbol{R}_k^3(i) + \boldsymbol{R}_k^4(i)$;
  end
end
return $\boldsymbol{R}_k$

Algorithm 3: Reallocation of unscheduled observation targets: function $[\boldsymbol{A}', \mathcal{U}] = Tar\_reallocation()$.

Input: The original target allocation result $\boldsymbol{A}$; the mission planning result $x_{i,k}$ of SA-JOTP
Output: The target reallocation result $\boldsymbol{A}'$; the set $\mathcal{U}$ of AEOSs that need to replanning missions

$\boldsymbol{A}' \leftarrow \boldsymbol{A}$; $\mathcal{U} \leftarrow \emptyset$;
for $i = 1 : N^a$ **do**
  for $k = 1 : N^o$ **do**
    if $(\boldsymbol{A}(k,i) - x_{i,k} \neq 0)$ *and* $(|\mathcal{V}_{I,k}^a| \geq 2)$ **then**
      $\boldsymbol{A}'(k,i) \leftarrow 0$;
      $\boldsymbol{R}_k \leftarrow Rank2(\boldsymbol{A}', \mathcal{V}_{I,k}^a \backslash \{i\})$;
      $\boldsymbol{A}'(k, \boldsymbol{R}_k(1)) \leftarrow 1$; // reallocate
      $\mathcal{U} \leftarrow [\mathcal{U}; \boldsymbol{R}_k(1)]$; // mark the AEOS
    end
  end
end
$\mathcal{U} \leftarrow unique(\mathcal{U})$; // remove duplicate elements
return $\boldsymbol{A}'$, $\mathcal{U}$

The target reallocation function is described in Algorithm 3, which named $[\boldsymbol{A}',\mathcal{U}] = Tar\_reallocation()$. In this algorithm, if target k is not scheduled and it has at least one other visible AEOS, then it can be reallocated. Here, function $Rank2()$ is the same as $Rank()$ except that $\boldsymbol{R}_k(i) \leftarrow \boldsymbol{R}_k^3(i) + \boldsymbol{R}_k^4(i)$ in step 15 of Algorithm 2. This is because the main goal of the reallocation is to make the observed targets as many as possible, so the number of allocated targets $\boldsymbol{R}_k^3(i)$ and the conflict degree $\boldsymbol{R}_k^4(i)$ are influential items, while the observation time $\boldsymbol{R}_k^1(i)$ and distance $\boldsymbol{R}_k^2(i)$ are not that important at this stage. In step 6 of Algorithm 3, we rank all AEOSs that can observe k except the original allocated AEOS i. Then, we reallocate k to the top-ranked AEOS in step 7 and mark this AEOS in step 8.

D. Distributed Algorithm for Multiple AEOSs

With the above mission allocation methods and the SA-JOTP model, we propose the MA-DJOTP algorithm for multiple AEOSs. The algorithm is described in Algorithm 4.

Firstly, in steps 1∼2, parameters are calculated based on the orbit information of satellites and the position of targets. Secondly in steps 3∼4, targets and CSs are allocated to their respective appropriate AEOSs by calling Algorithm 1 and solving the ILP problem (39)∼(42). Then, based on the allocation results, each AEOS can solve the SA-JOTP problem in parallel. Here in (4)∼(31) of the SA-JOTP, set $\mathcal{V}_{i,K}^o$ is replaced with $\{k|\boldsymbol{A}(k,i) = 1\}$, and set $\mathcal{V}_{i,J}^c$ is replaced with $\{j|\boldsymbol{C}(j,i) = 1\}$. With the mission planning result, we reallocate unscheduled targets to other AEOSs in step 8 by calling Algorithm 3. At last, for the AEOSs that have changed the target allocation results, they will solve the SA-JOTP problem again to realize more targets to be observed.

Assume the number of targets and CSs allocated to AEOS i are N_i^{oA} and N_i^{cA}, respectively. The number of targets reallocated to i is $N_i^{oA'}$. Then the complexity of the MA-DJOTP algorithm is discussed in Theorem 2.

Algorithm 4: A Distributed Joint Observation and Transmission Planning Algorithm for Multiple AEOSs: MA-DJOTP.

Input: The position of targets; the coordinate of CSs and AEOSs during the planning horizon;
Output: The observation and transmission planning results of all AEOSs;

1 Calculate the target visible matrix $\boldsymbol{O}_i$ and the ISL connectable matrix $\boldsymbol{S}_i$ of all AEOSs;
2 Obtain the sunlight parameter $l_{i,t}^s$ of all AEOSs;
3 $\boldsymbol{A} \leftarrow Tar\_allocation()$; `// Algorithm 1`
4 $\boldsymbol{C} \leftarrow Com\_allocation()$; `// Solve (39)∼(42)`
5 **for** $i = 1 : N^a$ **do** `// Solve in parallel`
6 Solve the SA-JOTP problem (31) with $k \in \{k|\boldsymbol{A}(k,i) = 1\}$ and $j \in \{j|\boldsymbol{C}(j,i) = 1\}$;
7 **end**
8 $[\boldsymbol{A}',\mathcal{U}] \leftarrow Tar\_reallocation()$; `// Algorithm 3`
9 **for** $\forall i \in \mathcal{U}$ **do** `// Solve in parallel`
10 Solve the SA-JOTP problem (31) with $k \in \{k|\boldsymbol{A}'(k,i) = 1\}$ and $j \in \{j|\boldsymbol{C}(j,i) = 1\}$;
11 **end**

Theorem 2. *The time complexity of the MA-DJOTP algorithm is upper bounded by* $O(2^{N_i^{oA}(T^o+T^c+1)+T^c(N_i^{cA}+1)+T^o+1})$.

Proof. The complexity of Algorithm 4 has four parts:

(a) Targets allocation in Algorithm 1. The complexity of first allocation and second allocation are $O(N^o)$ and $O(N^a)$. The rank of AEOSs in Algorithm 2 has the worst complexity of $O(N_k^a \cdot (N_i^{oA} - 1)) + O(N_k^a) = O(N_k^a \cdot N_i^{oA})$. Thus, the complexity of Algorithm 1 is upper bounded by $O(N^o) + O(N^a) + O(N^o \cdot N_k^a \cdot N_i^{oA}) \approx O(N^o \cdot N_k^a \cdot N_i^{oA})$.

(b) The CS allocation problem (39)∼(42). This ILP problem can be solved by the branch-and-bound (B&B) algorithm which has exponential complexity related to the number of integer variables in the worst case [18]. Thus, the complexity is upper bounded by $O(2^{N^c \cdot N^a})$.

(c) The SA-JOTP problem (31). This MIQCP problem can be solved by the branch-and-cut algorithm which combines the B&B and cutting plane algorithms [19]. In the worst case, it has exponential complexity since it involves a B&B tree. The number of integer decision variables $\boldsymbol{\psi}_i$, $x_{i,k}$, $p_{k,k'}$, $\boldsymbol{\delta}_i$, $\boldsymbol{\beta}_i$, $st_{i,k}$, $\xi_{i,t}$, $\lambda_{i,t}$ is $[N_i^o T^o + N_i^o + N_i^o(N_i^o - 1) + N_i^c T^c + N_i^o T^c + N_i^o + T^o + T^c] = N_i^o(T^o + T^c + 1) + T^c(N_i^c + 1) + T^o$. In Algorithm 4, steps 6 and 10 are solved in parallel. Thus, the complexity of steps 5∼7 and 9∼10 is upper bounded by $O(2^{N_i^{oA}(T^o+T^c+1)+T^c(N_i^{cA}+1)+T^o}) + O(2^{N_i^{oA'}(T^o+T^c+1)+T^c(N_i^{cA}+1)+T^o}) \approx O(2^{N_i^{oA}(T^o+T^c+1)+T^c(N_i^{cA}+1)+T^o+1})$.

(d) Target reallocation in Algorithm 3. The complexity is $O(N^a \cdot N^o)$.

Consequently, the complexity of the MA-DJOTP algorithm is upper bounded by $O(N^o \cdot N_k^a \cdot N_i^{oA}) + O(2^{N^c \cdot N^a}) + O(2^{N_i^{oA}(T^o+T^c+1)+T^c(N_i^{cA}+1)+T^o+1}) + O(N^a \cdot N^o) \approx O(2^{N_i^{oA}(T^o+T^c+1)+T^c(N_i^{cA}+1)+T^o+1})$. □

From Theorem 2, we can notice that the time complexity of the MA-DJOTP is influenced by the number of integer decision variables in SA-JOTP. Therefore, the task allocation of Algorithm 1 and the CS allocation of problem (39)∼(42) can reduce N_i^o and N_i^c to N_i^{oA} and N_i^{cA}, which contribute a lot to reducing the time complexity.

V. Simulation and Analysis

In this section, we verify the effectiveness of the proposed MA-DJOTP algorithm. Firstly, the parameter settings are introduced. Then, result analysis in a small system and algorithm performance in large systems are given with figures and tables.

A. Parameter Settings

We simulate the MCN with 720 CSs and four AEOS systems with different sizes. The small system has 3 AEOSs and the large systems have 16, 36, and 360 AEOSs, respectively. The orbit parameters of satellites in the four cases are listed in TABLE III. The CSs are in Walker-Star configuration referred to the OneWeb [4]. The AEOSs are in solar synchronous orbits with Walker-Delta configuration, and their orbit parameters are

TABLE III
ORBIT PARAMETERS OF SATELLITES.

System Cases		Small 1	Large 2	Large 3	Large 4
AEOS	Walker N/P/F	3/3/1	16/16/1	36/36/1	360/36/1
	Inclination (deg)	97.6			
	Altitude (km)	560			
CS	Walker N/P/F	720/18/10			
	Inclination (deg)	87.9			
	Altitude (km)	1200			

referred to the Shell 3 of Starlink [3]. We use the Satellite Tool Kit (STK) software to generate constellations and obtain their time-varying coordinates and sunlight information.

In the simulation, we consider AEOS AS-01 with the largest pitch degree of 45° and row degree of 45° [5]. We consider two scenarios of target distribution: 'W' represents worldwide distribution in 60°S-60°N and 180°W-180°E; 'A' represents Chinese area distribution in 3°N-53°N and 74°E-133°E. The number of targets ranges from 100 to 500. For example, '500_W' indicates a scenario with 500 targets of worldwide distribution.

We assume that each observation mission takes 30 seconds [15], so the time slot duration τ^o is set to 30s. The attitude transition time Δ^o is set to 60s [2], [7]. The ISL handover duration Δ^c is assumed to be 60 seconds [20], so the time slot duration τ^c is also 60s. The data amount q^o of each image is 10 Gbit, and the data rate v^c of ISL is 0.1 Gbit/s. The power of observation, attitude adjustment, laser acquisition, data transmission, and operation are set to $P^o = 0.6$kW, $P^a = 0.05$kW, $P^l = 0.1$kW, $P^t = 0.012$kW, $P^r = 0.1$kW, respectively [21]–[23]. The solar panels of each AEOS have an output power of $P^H = 3.2$kW, and the discharge depth of the battery is $\theta = 25\%$. The benefit ω_k of each target is randomly selected from the interval [1, 10]. According to Theorem 1, the weight values of objective function (31) are set to $\alpha_1 = 9$, $\alpha_2 = 1$. Other parameters, such as the target visible matrix $\boldsymbol{O}_i$, the link connectable matrix $\boldsymbol{S}_i$, and the sunlight duration $l^s_{i,t}$ are calculated based on the satellites' and targets' coordinates obtained from STK.

The simulation is executed on Dell 7080MT Optiplex with Intel(R) Core(TM) i7-10700 CPU@ 2.90GHz, 16 GB RAM with MATLAB R2022b on Windows 11. The Parallel Computing Toolbox in MATLAB is used for the parallel solving of the SA-JOTP problems in Algorithm 4. We solve the MIQCP and ILP problems in MA-DJOTP by solver Gurobi [24] and the modeling tool Yalmip [25].

B. Result Analysis in the Small System

In this subsection, we analyze the simulation results in the small system with 3 AEOSs.

1) State Diagram in Time Domain: To verify the effectiveness of the observation and transmission planning result, we show a state diagram of a certain AEOS in a 500_W scenario in Fig. 3. The planning horizon is set as the orbital period of the AEOS, which is 96 minutes. The AEOS has four states:

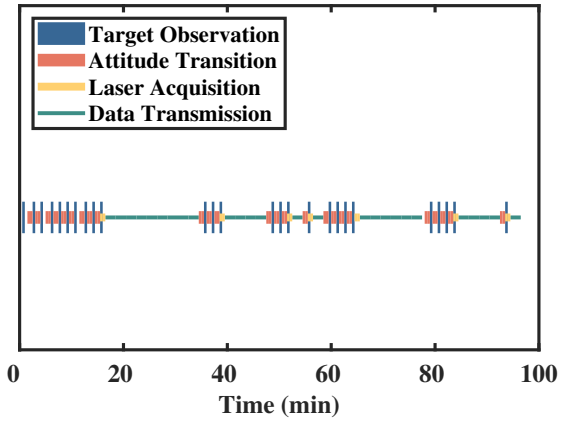

Fig. 3. State diagram in the time domain of a certain AEOS in 500_W scenario (planning horizon = 96 min).

target observation, attitude transition, laser acquisition, and data transmission. It can be seen that the four operations are arranged appropriately in the time domain, which is consistent with the proposed optimization model (31):

- Enough attitude transition time before observing targets.
- Enough laser acquisition time before data transmission.
- Laser acquisition and data transmission are not performed during the attitude transition.
- ISLs' continuity is maintained as much as possible.

2) Result Comparison with the Centralized Method: The centralized method is to plan the observation and transmission missions by taking all targets, AEOSs, and CSs in one optimization problem, which can obtain the global optimum. Compared to the SA-JOTP model (31), the centralized method has two other constraints:

$$\sum_{i=1}^{N^a} \boldsymbol{\delta}_i(j,t) \le 1 \quad \forall j \in [1, N^c],\ \forall t \in \mathcal{T}^c \tag{43}$$

$$\sum_{i=1}^{N^a} x_{i,k} \le 1 \quad \forall k \in [1, N^o] \tag{44}$$

where (43) guarantees each CS can only connect to one AEOS at each time slot, (44) constrains each target can be observed at most once. The objective of the centralized method is the sum of (31) for $i \in [1, N^a]$.

Fig. 4 shows the comparison of MA-DJOTP and the centralized method in benefits and solving time. From (a) and (c), we can see that the total benefit of MA-DJOTP is very close to the global optimum obtained by the centralized method. It indicates that MA-DJOTP can obtain excellent results with varying planning horizons and different numbers of targets. From (b) and (d), we can see that the solving time of MA-DJOTP increases slowly with the increase of the problem scale, while the solving time of the centralized method increases sharply. Therefore, the centralized method is not applicable in large constellation systems since the problem is too huge to be solved. Consequently, MA-DJOTP can obtain a solution very close to the global optimum in much less time than the centralized method.

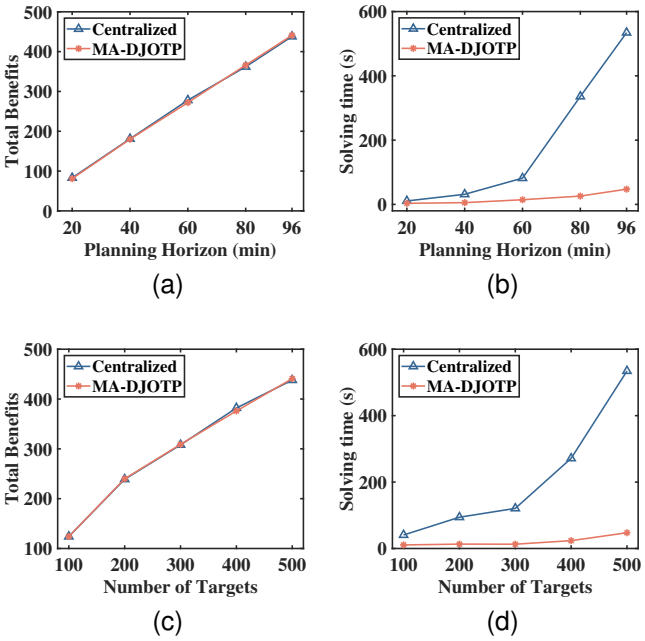

Fig. 4. Comparison of MA-DJOTP with the centralized method in small system with worldwide target distribution. (a) Benefits vs. Planning horizon (500_W); (b) Solving time vs. Planning horizon (500_W); (c) Benefits vs. Number of targets (planning horizon = 96 min); (d) Solving time vs. Number of targets (planning horizon = 96 min).

3) Effects of Energy and Storage Resources: The onboard resources of AEOSs have effects on the obtained benefits. Fig. 5 shows the total benefits under varying energy capacity $E_i^{\max}$ and memory capacity $B_i^{\max}$. It can be seen that the benefits increase as the memory capacity increases below 128Gbit, and as the energy capacity increases below 1500kJ. This is because when the memory capacity is limited, the observation data that can be stored is limited, so increasing memory can obtain more benefits. Similarly, when the energy capacity is limited, the missions that can be performed by AEOSs are limited, so increasing energy can obtain more benefits. However, when the memory and energy are sufficient, the observed targets and transmitted data reach the upper limit due to the planning horizon and number of targets, so the benefit no longer increases.

C. Algorithm Performance in Different Sizes of Systems

In this subsection, we verify the algorithm's effectiveness in different sizes of constellation systems.

1) Solving Time in Different Scenarios: We compare the solving time of MA-DJOTP in scenarios 500_W, 100_A, and 100_W with varying numbers of AEOSs in Fig. 6. Generally, the solving time has the relation: 500_W>100_A>100_W. It indicates that more targets and a smaller target distribution range can both make the problem more complex and need more time to be solved. An unusual finding is that in 500_W, the solving time does not increase linearly as the number of AEOSs increases. This is because when there are 16 AEOSs and 500 targets, each AEOS would be allocated lots of targets, so the solving of the SA-JOTP problem will be more complex

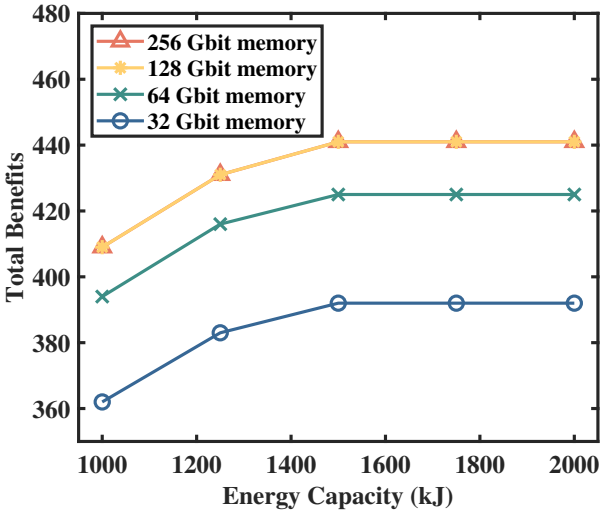

Fig. 5. Total benefits with different energy capacity $E_i^{\max}$ and memory capacity $B_i^{\max}$ (target scenario: 500_W, planning horizon = 96 min).

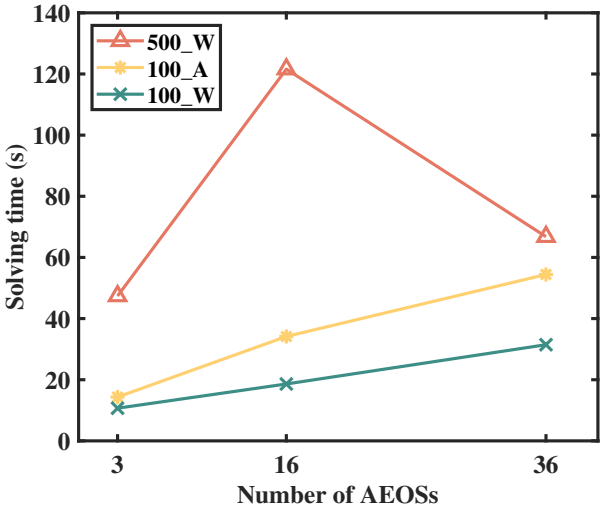

Fig. 6. Solving time with different number of AEOSs in targets scenarios 500_W, 100_A, and 100_W (planning horizon = 96 min).

to select high-benefit targets to be observed and transmit data in the limited planning horizon. With 36 AEOSs, each AEOS would not be allocated too many targets, so the mission planning of each AEOS will be more easier. In general, the solving time performance of MA-DJOTP is excellent under varying numbers of AEOSs and target distribution scenarios.

2) Indicators Analysis and Algorithms Comparison: We compare the simulation results of MA-DJOTP with the JOTSAS algorithm proposed in [15]. The differences between JOTSAS and MA-DJOTP are listed in TABLE I. In this subsection, we analyze four indicators as follows:

- Abenefit: Average benefits of each AEOS.
- Adelay: Average transmission delay (in minutes), where the transmission delay of each target k is calculated by $(st_{i,k} - \sum_{t\in\mathcal{T}^o}[\psi_i(k,t)\cdot t])$.
- vNum: The total number of visible targets of all AEOSs

TABLE IV
INDICATORS ANALYSIS AND ALGORITHMS COMPARISON

Algorithms	JOTSAS	MA-DJOTP					
Scenarios	100_W	100_W		100_A		500_W	
AEOS' number	3	3	36	3	36	3	36
Abenefit	40.67	41.33	14.28	22.33	13.17	147	76.69
Adelay (min)	18.16	2.43	1.16	14.88	7.59	10.35	3.71
vNum	25	25	100	23	100	99	500
oNum	22	23	100	8	82	66	499

within the planning horizon.

- oNum: The total number of observed targets.

The indicators of JOTSAS and MA-DJOTP under different scenarios with the planning horizon of 96 minutes are listed in TABLE IV. We only list the result of JOTSAS in 100_W with 3 AEOSs here, because the other cases can not be solved by JOTSAS within 60 hours due to the centralized model and the complex modeling of transition time constraints.

From TABLE IV, several conclusions can be obtained as:

- JOTSAS can not obtain the optimal number of observed targets and benefits as MA-DJOTP, because some unnecessary transition time in the JOTSAS. Besides, targets' data need to wait for a long time for transmission since JOTSAS does not consider the second objective of (31).
- As for benefits: 1) in the same targets scenario, the more AEOSs, the less average benefit of each AEOS; 2) with the same number of AEOSs and targets, the smaller the range of targets distribution, the less benefits; 3) with the same number of AEOSs and targets distribution range, the more targets, the more benefits.
- As for transmission delay: 1) in the same target scenario, the more AEOSs, the shorter the transmission delay for each target; 2) with the same number of AEOSs, the denser the target distribution, the longer the transmission delay.
- As for observed targets: the denser the target distribution, the smaller the rate of oNum/vNum.

3) Effectiveness in Mega Constellation Networks: We verify the algorithm performance in MCN with 360 AEOSs and 720 CSs in Fig. 7. It can be seen that in 10 minutes, the 360 AEOSs can observe 463 targets and transmit their data, and the solving time is only 41.04 seconds. All targets can be observed and transmitted data in 30 minutes, and the solving time is at the minute level. The result indicates that MA-DJOTP has fast mission planning capability for the entire MCN, which can effectively deal with some emergencies.

VI. CONCLUSION

In this paper, we propose a distributed joint observation and transmission planning algorithm for multiple AEOSs (i.e. MA-DJOTP) in MCNs. This algorithm uses a targets allocation strategy, a CS allocation model, and a targets reallocation strategy to transform the multi-AEOS problem into several single-AEOS subproblems and solve them in parallel. For each AEOS, a joint observation and transmission planning model (i.e. SA-JOTP) is formulated as an MIQCP problem

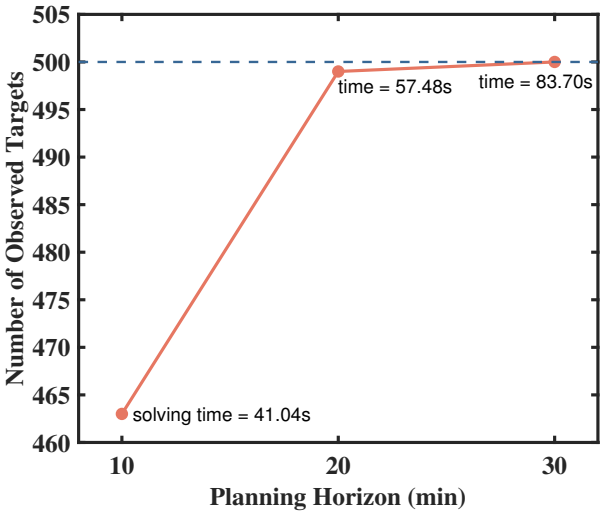

Fig. 7. Number of observed targets in mega constellation network with 360 AEOSs (target scenario: 500_W).

based on a mission-based time slot division method, which can help simplify the OTW determination and ISL handover time modeling. The SA-JOTP model can realize both the benefit maximization and transmission delay minimization based on practical constraints of mission transition time, laser ISLs' characteristics, and limited onboard resources. We verify the effectiveness of MA-DJOTP in MCNs with 720 CSs and 3, 16, 36, 360 AEOSs. The results show that the proposed algorithm can arrange AEOSs' observation and transmission missions effectively in the time domain. The onboard energy and storage capacity can both affect the optimal solution of benefits. The MA-DJOTP algorithm can obtain a solution close to the global optimum of the centralized method and has minute-level solving time in different target scenarios and hundreds of satellites. Compared to JOTSAS in the existing research, the proposed MA-DJOTP shows great application potential in MCNs.

In the future, we will study the multi-AEOS collaborative mission planning problem and consider some other observation modes for different target shapes and imaging requirements.

REFERENCES

[1] L. Zhao, Q. Zhang, Y. Li, Y. Qi, X. Yuan, J. Liu, and H. Li, "China's gaofen-3 satellite system and its application and prospect," *IEEE Journal of Selected Topics in Applied Earth Observations and Remote Sensing*, vol. 14, pp. 11 019–11 028, 2021.

[2] G. Peng, G. Song, Y. He, J. Yu, S. Xiang, L. Xing, and P. Vansteenwegen, "Solving the agile earth observation satellite scheduling problem with time-dependent transition times," *IEEE Transactions on Systems, Man, and Cybernetics: Systems*, vol. 52, no. 3, pp. 1614–1625, Mar. 2022.

[3] "Starlink: World's most advanced broadband satellite internet," SpaceX, 2024. [Online]. Available: https://www.starlink.com/technology

[4] "Oneweb: Space is the future," OneWeb, 2024. [Online]. Available: https://oneweb.net/

[5] X. Liu, G. Laporte, Y. Chen, and R. He, "An adaptive large neighborhood search metaheuristic for agile satellite scheduling with time-dependent transition time," *Computers & Operations Research*, vol. 86, pp. 41–53, Apr. 2017.

[6] G. Peng, R. Dewil, C. Verbeeck, A. Gunawan, L. Xing, and P. Vansteenwegen, "Agile earth observation satellite scheduling: An orienteering problem with time-dependent profits and travel times," *Computers & Operations Research*, vol. 111, pp. 84–98, Nov. 2019.

[7] C. Han, Y. Gu, G. Wu, and X. Wang, "Simulated annealing-based heuristic for multiple agile satellites scheduling under cloud coverage uncertainty," *IEEE Transactions on Systems, Man, and Cybernetics: Systems*, vol. 53, no. 5, pp. 2863–2874, May 2023.

[8] Y. He, L. Xing, Y. Chen, W. Pedrycz, L. Wang, and G. Wu, "A generic markov decision process model and reinforcement learning method for scheduling agile earth observation satellites," *IEEE Transactions on Systems, Man, and Cybernetics: Systems*, vol. 52, no. 3, pp. 1463–1474, Mar. 2022.

[9] Y. Du, T. Wang, B. Xin, L. Wang, Y. Chen, and L. Xing, "A data-driven parallel scheduling approach for multiple agile earth observation satellites," *IEEE Transactions on Evolutionary Computation*, vol. 24, no. 4, pp. 679–693, Aug. 2020.

[10] D. Zhou, M. Sheng, X. Wang, C. Xu, R. Liu, and J. Li, "Mission aware contact plan design in resource-limited small satellite networks," *IEEE Transactions on Communications*, vol. 65, no. 6, pp. 2451–2466, Jun. 2017.

[11] Z. Yan, G. Gu, K. Zhao, Q. Wang, G. Li, X. Nie, H. Yang, and S. Du, "Integer linear programming based topology design for GNSSs with inter-satellite links," *IEEE Wireless Communications Letters*, vol. 10, no. 2, pp. 286–290, Feb. 2021.

[12] Z. Yan, K. Zhao, W. Li, C. Kang, J. Zheng, H. Yang, and S. Du, "Topology design for GNSSs under polling mechanism considering both inter-satellite links and ground-satellite links," *IEEE Transactions on Vehicular Technology*, vol. 71, no. 2, pp. 2084–2097, Feb. 2022.

[13] N. Guo, L. Liu, and X. Zhong, "Task-aware distributed inter-layer topology optimization method in resource-limited LEO-LEO satellite networks," *IEEE Transactions on Wireless Communications*, pp. 1–1, Sep. 2023.

[14] J. Zhang and L. Xing, "An improved genetic algorithm for the integrated satellite imaging and data transmission scheduling problem," *Computers & Operations Research*, vol. 139, p. 105626, Mar. 2022.

[15] L. He, B. Liang, J. Li, and M. Sheng, "Joint observation and transmission scheduling in agile satellite networks," *IEEE Transactions on Mobile Computing*, vol. 21, no. 12, pp. 4381–4396, Dec. 2022.

[16] J. Löfberg, "Logics and integer-programming representations," Jekyll & Minimal Mistakes, Sep. 2016. [Online]. Available: https://yalmip.github.io/tutorial/logicprogramming

[17] K. Deb, K. Sindhya, and J. Hakanen, "Multi-objective optimization," in *Decision sciences*. CRC Press, 2016, pp. 161–200.

[18] D. R. Morrison, S. H. Jacobson, J. J. Sauppe, and E. C. Sewell, "Branch-and-bound algorithms: A survey of recent advances in searching, branching, and pruning," *Discrete Optimization*, vol. 19, pp. 79–102, Feb. 2016.

[19] J. Zhang, C. Liu, X. Li, H.-L. Zhen, M. Yuan, Y. Li, and J. Yan, "A survey for solving mixed integer programming via machine learning," *Neurocomputing*, vol. 519, pp. 205–217, Jan. 2023.

[20] M. Gregory, F. Heine, H. Kämpfner, R. Meyer, R. Fields, and C. Lunde, "Tesat laser communication terminal performance results on 5.6 Gbit coherent inter satellite and satellite to ground links," in *International Conference on Space Optics—ICSO 2010*, vol. 10565. SPIE, Nov. 2017, pp. 324–329.

[21] X. Wang, G. Song, R. Leus, and C. Han, "Robust earth observation satellite scheduling with uncertainty of cloud coverage," *IEEE Transactions on Aerospace and Electronic Systems*, vol. 56, no. 3, pp. 2450–2461, Jun. 2020.

[22] X. Chen, X. Chen, L. Cao, X. Zhang, and W. Yao, "Integrated optimization design method of satellite overall system and attitude control (in chinese)," *Journal of Astronautics*, vol. 44, no. 4, pp. 465–475, Apr. 2023.

[23] D. Gao, T. Li, Y. Sun, W. Wang, H. Hu, J. Meng, Y. Zheng, and X. Xie, "Latest developments and trends of space laser communication (in chinese)," *Chinese Optics*, vol. 11, no. 6, pp. 901–913, Dec. 2018.

[24] "Gurobi optimization, solve complex problems, fast," GUROBI OPTIMIZATION, LLC., 2024. [Online]. Available: https://www.gurobi.com

[25] J. Löfberg, "Yalmip," Jekyll & Minimal Mistakes, 2024. [Online]. Available: https://yalmip.github.io/